Four-quadrant Zero-voltage-transition Converter-fed DC Motor Drives for Electric Propulsion

T. W. Ching

Department of Electromechanical Engineering, University of Macau, twching@umac.mo

Abstract

In this paper, a new four-quadrant (4Q) soft-switching converter for dc motor drives, namely the 4Q zero-voltage-transition (4Q-ZVT) converter, is proposed. It has some definite advantages over their hard-switching counterparts and other soft-switching converters. It offers zero-voltage-switching (ZVS) for all main switches and diodes, as well as unity device voltage and current stresses. It also has simple circuit topology, hence minimum hardware count and low cost.

Keywords

soft-switching, zero-voltage-transition, DC motor

1. INTRODUCTION

Traditionally, dc commutator motors have been loosely named as dc motors. Their control principle is simple because of the orthogonal disposition of field and armature MMFs. Because of mature technology and simple control, dc motors have ever been prominent in electric propulsion. Actually, various types of dc motors, including series, shunt, separately excited and permanent magnet excited, have been adopted by recent electric vehicles (EVs). For example, the dc series motor in the Daihatsu Hijet and Fiat 500 Elettra, the dc shunt motor in the Mazada Bongo, the dc separately excited motor in the Fiat 900E/E2, and the PM dc motor in the Suzuki Senior Tricycle [Chan, 2004]. PM dc motors are sometimes used for low-power applications, e.g. golf carts and motorcycles. It is probable that dc motors of less than 20kW will continue to be used for small city cars owing to their easy control feature and excellent dynamic performance and low cost and efficient chopper control of armature and shunt field currents.

As regenerative braking is very essential for EVs which can extend the vehicle driving range by up to 12% [Rajashekara 1994]. The two-quadrant (2Q) dc chopper (see Figure 1(a)) is preferred as it converts battery dc voltage to variable dc voltage during the motoring mode and revert the power flow during regenerative braking. Furthermore, four-quadrant (4Q) dc choppers (see Figure 1(b)) are employed for reversible and regenerative speed control of dc motors. Instead of using mechanical contactors to achieve reversible operation, the four-quadrant dc chopper can be employed so that motoring and regenerative braking in both forward and reversible operations are controlled electronically. Both 2Q and 4Q dc choppers are shown in Figure 2.

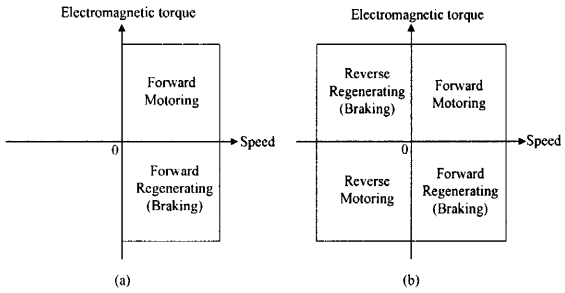

Fig. 1 Operation of a dc motor : (a) 2Q; (b) 4Q

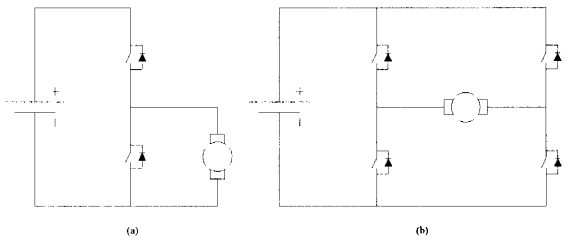

Fig. 2 Conventional dc choppers : (a) 2Q; (b) 4Q

Soft-switching converters for EV propulsion are recently receiving wide attention in the literature [Chan et al., 2001]. However, soft-switching dc-dc converters are seldom used for voltage control of dc motor drives. The major reason is due to the fact that the corresponding development has been much less than that for switched-mode power supplies. Also, those available soft-switching dc-dc converters cannot handle backward power flow during regenerative braking. Until recently, two 2Q soft-switching dc-dc converters have been developed, namely the 2Q zero-voltage transition (2Q-ZVT) converter [Chau et al., 1999], and the 2Q zero-current transition (2Q-ZCT) converter [Ching et al., 2001] for dc motor drives, which possess the advantages of high efficiency for both motoring and regenerative braking. Following this spirit, the purpose of this paper is to propose a new

4Q-ZVT converter for electric propulsion.

2. PROPOSED 4Q-ZVT CONVERTER

Figure 3 shows the schematic diagram of the proposed 4Q-ZVT converter for dc motor drives. To achieve ZVT operation, there are two resonant tanks. First, a resonant inductor L_a, resonant capacitors $C_a/2$, auxiliary switches S_a and $S_{a'}$ are added to allow for soft switching S1 and S_4. Second, resonant inductor L_b, resonant capacitors $C_b/2$, auxiliary switches S_b and $S_{b's}$ are added to allow for soft switching S_2 and S_3. The dc motor can be considered to be simultaneously fed by two 2Q-ZVT converters.

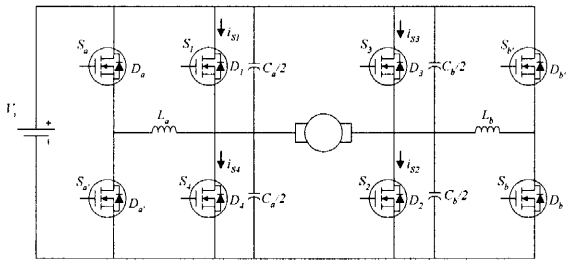

Fig. 3 Proposed 4Q-ZVT converter

The proposed ZVT converter operates in four modes (Figure 1(b)) :

- Forward motoring mode (Figures 4 to 6),
- Forward regenerating mode (Figures 7 to 9),
- Reverse motoring mode (Figures 10 to 12), and
- Reverse regenerating mode (Figures 13 to 15).

Their corresponding equivalent circuits and operating waveforms are shown in Figures 4 to 15. It can be found that all equivalent circuits involve seven operating stages (S1 to S7) within one switching cycle.

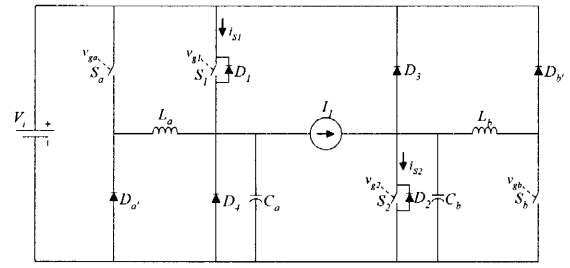

Fig. 4 Equivalent circuit during forward motoring mode

2.1 Forward motoring operation of ZVT converter

(see Figures 4 to 6)

(a) Stage 1 [T_0-T_1]: I_1 is freewheeling via D_3 and D_4.

(b) Stage 2 [T_1-T_2]: S_a and Sb are turned on respectively. Then I_{La} and L_{Lb} increase linearly. This stage finishes at T_2 when i_{La} and i_{Lb} equals to I_1.

(c) Stage 3 [T_2-T_3] : When i_{La} and i_{Lb} equal to I_1, D_3 and D_4 are turned off with ZVS, and L_a, C_a and L_b, C_b start resonating. This stage ends at T_3 when v_{Ca} and v_{Cb} equal V_g.

(d) Stage 4 [T_3-T_4]: When v_{Ca} and v_{Cb} reach V_g, S_1 and S_2 are turned on with ZVS. S_a and S_b are turned off to recover the stored energy in L_a and L_b to the source. Then i_{La} (i_{Lb}) flows through $D_{a'}$ ($D_{b'}$) and decreases linearly. At T_4, i_{La} (i_{Lb}) decreases to I_1 and i_{S1} (i_{S2}) crosses zero from negative to positive.

(e) Stage 5 [T_4-T_5]: i_{La} (i_{Lb}) keeps decreasing while i_{S1}

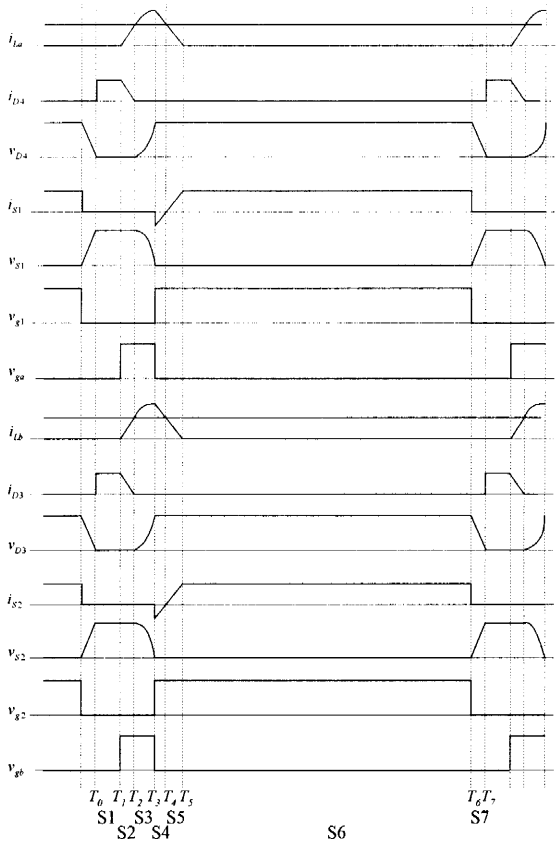

Fig. 5 Key waveforms during forward motoring mode

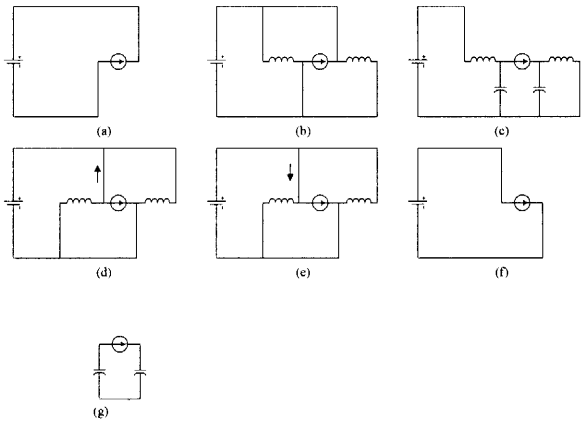

Fig. 6 Seven topological stages during forward motoring mode

(i_{S2}) increasing until i_{La} (i_{Lb}) reaches zero at T_5 and $D_{a'}$ ($D_{b'}$) becomes off.

(f) Stage 6 [T_5-T_6]: It is a forward powering stage. V_g is directly connected to I_1 via S_1 and S_2.

(g) Stage 7 [T_6-T_7]: I_1 discharges C_a and C_b linearly until v_{Ca} (v_{Cb}) equals zero at T_7, and eventually D_3 and D_4 become turn-on with ZVS.

2.2 Forward regenerating operation of ZVT converter

(see Figures 7 to 9)

(a) Stage 1 [T_0-T_1]: D_1 and D_2 are conducting, and it is a regenerating stage.

(b) Stage 2 [T_1-T_2]: $S_{a'}$ is turned on. i_{La} increases linearly. This stage finishes at T_2 when i_{La} equals I_2.

(c) Stage 3 [T_2-T_3]: When i_{La} reaches I_2 at T_2, D_1 becomes turn-off with ZVS, and L_a and C_b start resonating. At T_3, v_{Ca} decreases to zero.

(d) Stage 4 [T_3-T_4]: When v_{Ca} reaches zero, S_4 is turned on with ZVS. $S_{a'}$ is turned off to recover the stored energy in L_a to the source. Then i_{La} flows through $D_{a'}$ and decreases linearly. At T_4, i_{La} decreases to I_2 and i_{S4} crossed zero from negative to positive.

(e) Stage 5 [T_4-T_5]: i_{La} keeps decreasing and i_{S4} increasing until i_{La} reaches zero at T_5. D_a become off.

(f) Stage 6 [T_5-T_6]: I_2 is freewheeling.

(g) Stage 7 [T_6-T_7]: I_2 charges C_a linearly until v_{Ca} equals V_g at T_7, and eventually D_1 becomes turn-on with ZVS.

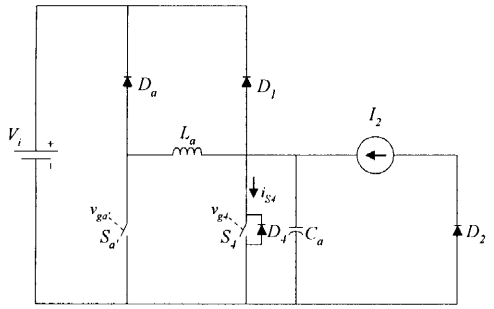

Fig. 7 Equivalent circuit during forward regenerating mode

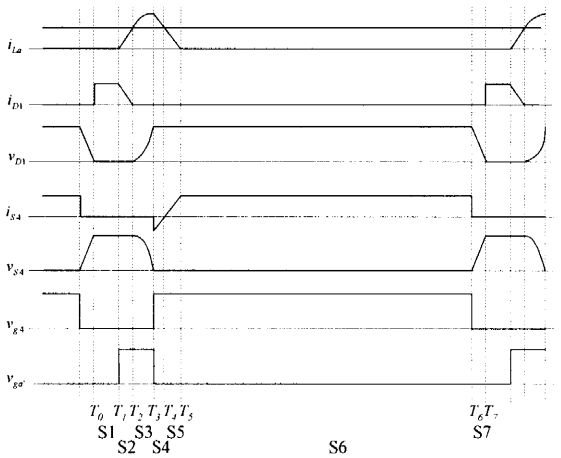

Fig. 8 Key waveforms during forward regenerating mode

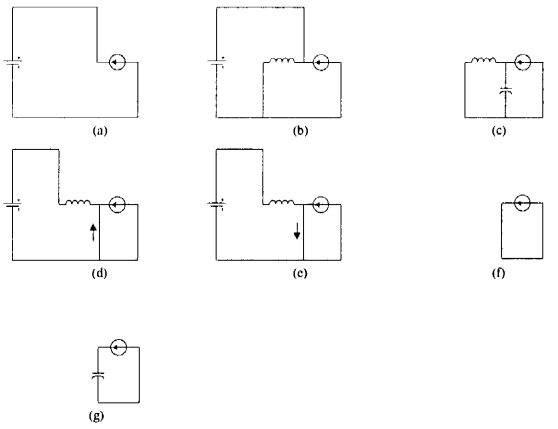

Fig. 9 Seven topological stages during forward regenerating mod

2.3 Reverse motoring operation of ZVT converter

(see Figures 10 to 12)

(a) Stage 1 [T_0-T_1]: I_3 is freewheeling via D_1 and D_2.

(b) Stage 2 [T_1-T_2]: $S_{a'}$ and $S_{b'}$ are turned on respectively. Then i_{La} and i_{Lb} increase linearly. This stage finishes at T_2 when i_{La} and i_{Lb} equals to I_3.

(c) Stage 3 [T_2-T_3]: When i_{La} and i_{Lb} equals to I_3, D_1 and D_2 are turned off with ZVS, and L_a, C_a and L_b, C_b start resonating. This stage ends at T_3 when v_{Ca} and v_{Cb} equals V_g.

(d) Stage 4 [T_3-T_4]: When v_{Ca} and v_{Cb} reach V_g, S_3 and S_4 are turned on with ZVS. $S_{a'}$ and $S_{b'}$ are turned off to recover the stored energy in L_a and L_b to the source. Then i_{La} (i_{Lb}) flows through D_a (D_b) and decreases linearly. At T_4, i_{La} (i_{Lb}) decreases to I_3 and i_{S3} (i_{S4}) crosses zero from negative to positive.

(e) Stage 5 [T_4-T_5]: i_{Lb} (i_{Lb}) keeps decreasing while i_{S3} (i_{S4}) increasing until i_{La} (i_{Lb}) reaches zero at T_5 and D_a (D_b) becomes off.

(f) Stage 6 [T_5-T_6]: It is a reverse powering stage. V_g is directly connected to I_3 via S_3 and S_4.

(g) Stage 7 [T_6-T_7]: I_3 discharges C_a and C_b linearly until v_{Ca} (v_{Cb}) equals zero at T_7, and eventually D_1 and D_2 become turn-on with ZVS.

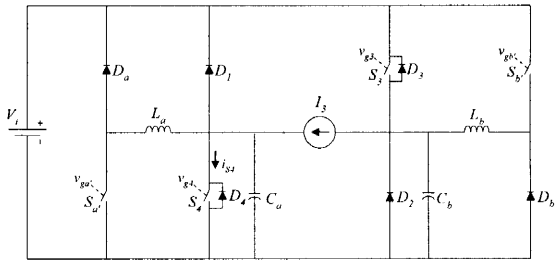

Fig. 10 Equivalent circuit during reverse motoring mode

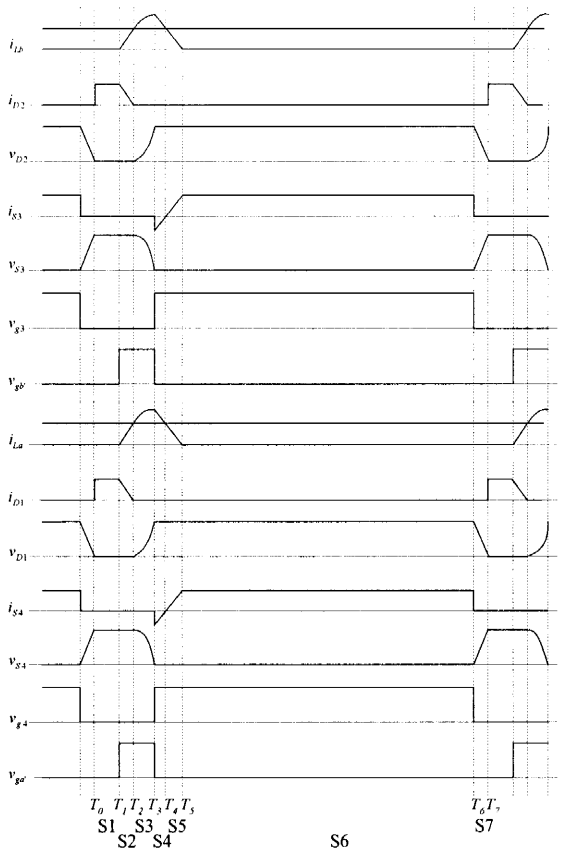

Fig. 11 Key waveforms during reverse motoring mode

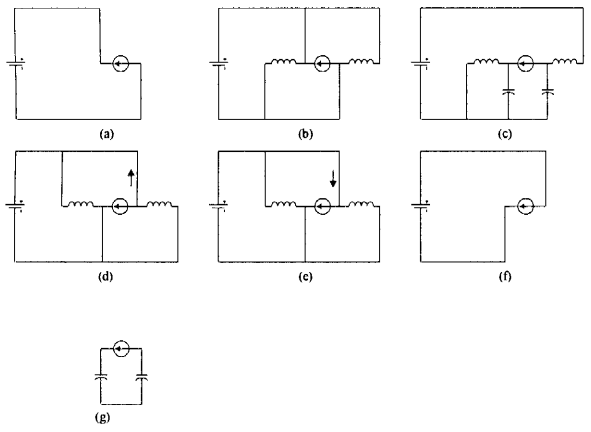

Fig. 12 Seven topological stages during reverse motoring mode

2.4 Reverse regenerating operation of ZVT converter

(see Figures 13 to 15)

(a) Stage 1 [T_0 -T_1]: I_4 is regenerating via D_3 and D_4.

(b) Stage 2 [T_1- T_2]: $S_{b'}$ is turned on. Then i_{Lb} increase linearly. This stage finishes at T_2 when i_{Lb} equals to I_4.

(c) Stage 3 [T_2-T_3]: When i_{Lb} equals to I_4, D_3 is turned off with ZVS, L_b and C_b start resonating. This stage ends at T_3 when v_{Cb} equals .

(d) Stage 4 [T_3-T_4]: When v_{Cb} reaches V_g, S_2 is turned on with ZVS. $S_{b'}$ is turned off to recover the stored energy in L_b to the source. Then i_{Lb} flows through D_b and decreases linearly. At T_4, i_{Lb} decreases to I_4 and i_{S2} crosses zero from negative to positive.

(e) Stage 5 [T_4-T_5]: i_{Lb} keeps decreasing while i_{S2} increasing until i_{Lb} reaches zero at T_5 and D_b becomes off.

(f) Stage 6 [T_5-T_6]: It is a freewheeling.

(g) Stage 7 [T_6-T_7]: I_4 discharges C_b linearly until v_{Cb} equals zero at T_7, and eventually D_3 become turn-on with ZVS.

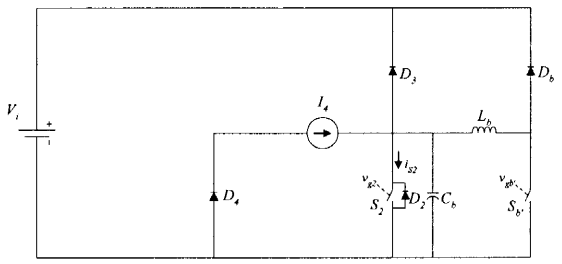

Fig. 13 Equivalent circuit during reverse regenerating mode

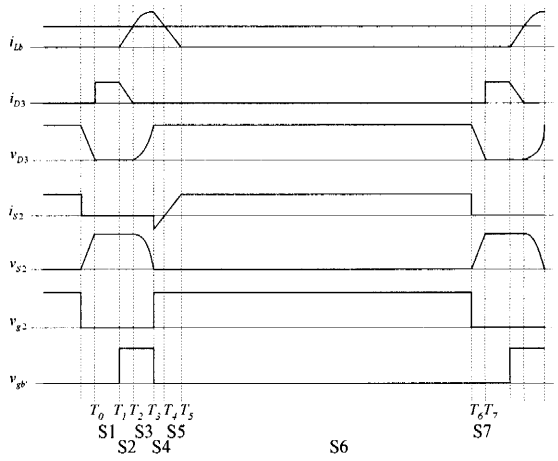

Fig. 14 Key waveforms during reverse regenerating mode

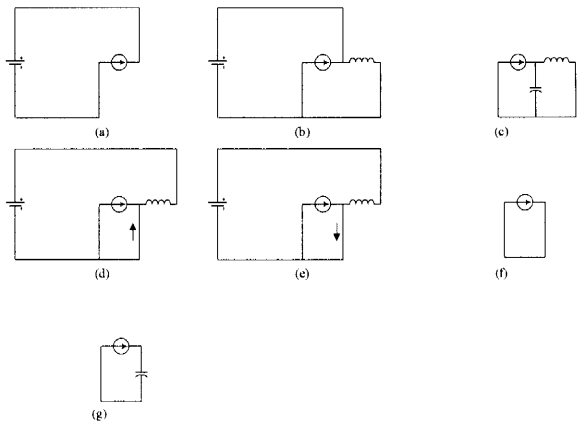

Fig. 15 Seven topological stages during reverse regenerating mode

3. SIMULATION AND EXPERIMENT

Different modes of operation of the proposed 4Q-ZVT converter are PSpice-simulated. The corresponding results are shown in Figures 16 to 19.

Figure 16 shows the simulated waveforms of the proposed converter operating in the forward motoring mode. Both S_a and S_b are switched together to allow soft switching S_1 and S_2.

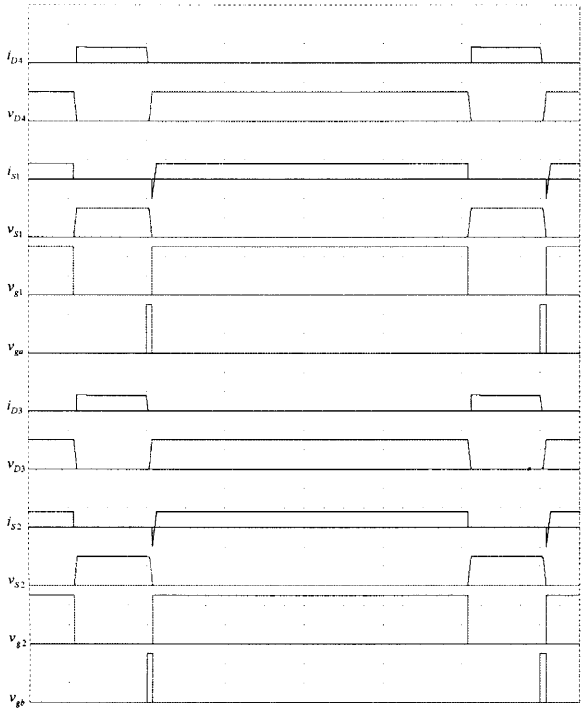

Fig. 16 PSpice simulation at forward motoring mode

Operating waveforms of the 4Q-ZVT converter operating in forward regenerating (braking) mode is shown in Figure 17.

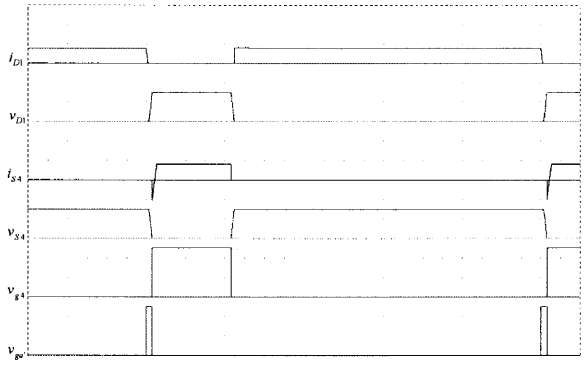

Fig. 17 PSpice simulation at forward regenerating mode

Operating waveforms of the 4Q-ZVT converter operating in reverse motoring mode is shown in Figure 18. Both $S_{a'}$ and $S_{b'}$ are switched together to allow soft switching S_3 and S_4.

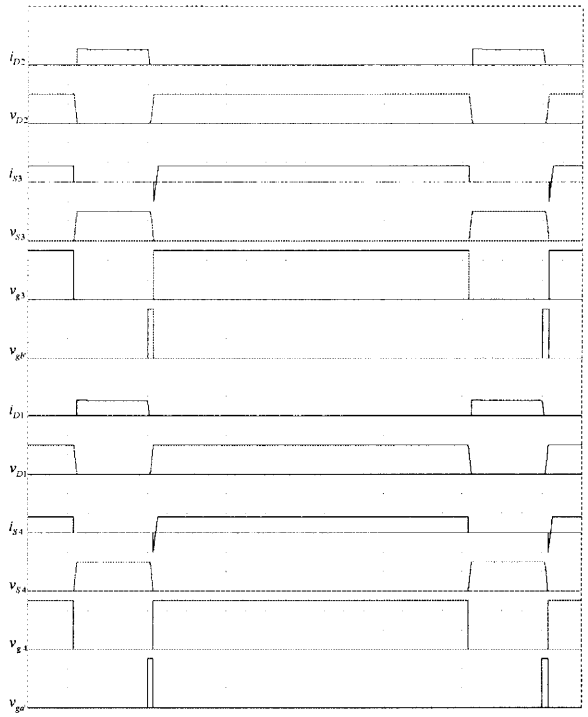

Fig. 18 PSpice simulation at reverse motoring mode

Operating waveforms of the 4Q-ZVT converter operating in reverse regenerating (braking) mode is shown in Figure 19.

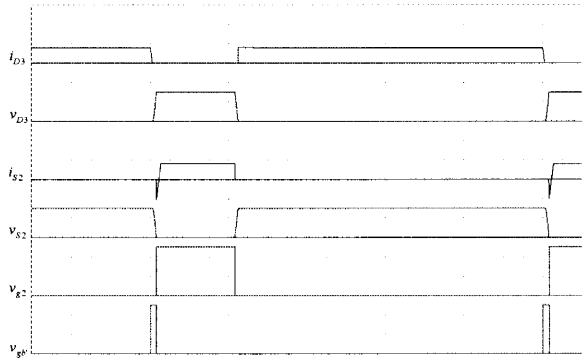

Fig. 19 PSpice simulation at reverse regenerating mode

The simulation results agree with those theoretical waveforms. The main switches and diodes of the converter can always maintain ZVS operation, and they are subjected to the same voltage and current stresses as those in the PWM counterpart. Nevertheless, the four auxiliary switches still suffer from hard-switching operation. Since the power involved in these auxiliary switches is only a fraction of the total power handled by the main switches, the hard-switching turn-off losses of the auxiliary circuitry can be out-weighted by the reduction of switching losses in the main circuitry.

To verify the theoretical results, the ZVT-4Q converter is hardware prototyped as shown in Figure 20.

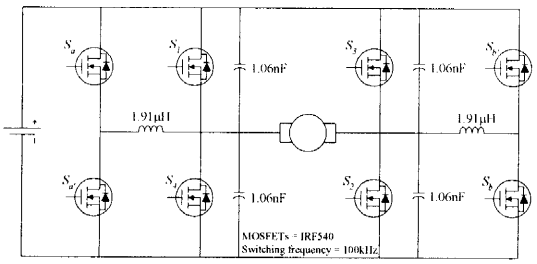

Fig. 20 Experimental ZVT-4Q converter fed DC motor drive

From the experimental waveforms shown in Figures 21 and 22, they closely agree with those theoretical waveforms, especially the main switches ($S_{1\text{-}4}$ and $D_{1\text{-}4}$ for motoring while S_2, S_4, D_1 and D_3 for regenerating) can always maintain ZVS operation.

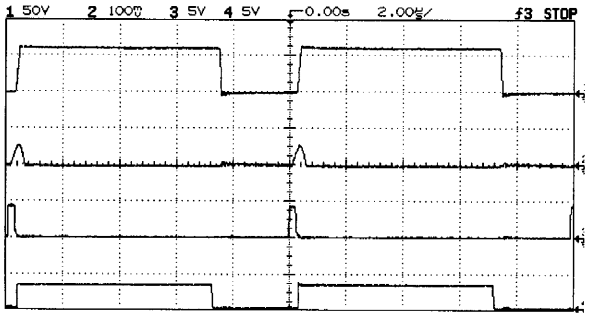

Fig. 21 Measured key waveforms at motoring (Duty Ratio=0.7); v_{D4} (50V/div); i_{La} (10A/div), v_{ga}, v_{g1} (5V/div).

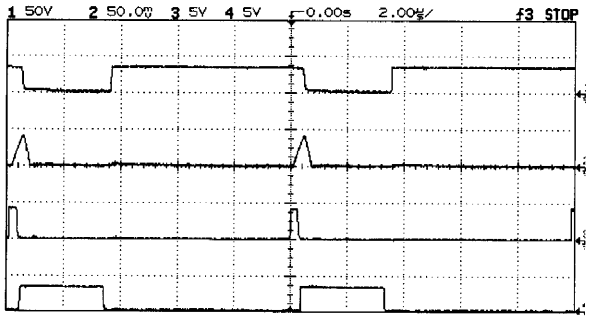

Fig. 22 Measured key waveforms at regenerating (Duty Ratio=0.3); v_{S4} (50V/div); i_{La} (5A/div), v_{ga}, v_{g4} (5V/div)

Comparing with its hard-switching counterpart (by removing the auxiliary resonant branches), the efficiency of the proposed converter is improved by 2-3% and 1-2% for motoring and regenerating modes respectively. Moreover, as shown in Figure 23, the measured efficiency (η) of the proposed converter is quite high, ranging from 94% to 98%.

4. CONCLUSION

The principle of operation, characteristics, design example, computer simulation and experimental results of a new ZVT-2Q converter for dc motor drives has been

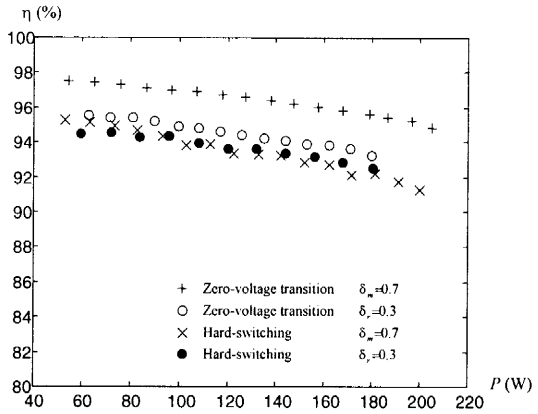

Fig. 23 Measured efficiency (η) at both motoring and regenerating

presented. It possesses some definite advantages, including ZVS for all main switches and diodes, unity device voltage and current stresses, simple circuit topology and low cost, leading to achieve high switching frequency, high power density and high efficiency for both motor and regenerative braking. Other key features are the use of the same resonant tank for both forward and backward power flows and the full utilization of all built-in diodes of the power switches, thus minimizing the overall hardware count and cost.

References

Chan, C. C., and K. T. Chau, *Modern Electric Vehicle Technology*, Oxford University Press, 2001.

Chan, C.C., The State of the art of electric vehicles, *Journal of Asian Electric Vehicles*, Vol. 2, No. 2, 579-600, 2004.

Chau, K. T., T. W. Ching, and C. C. Chan, A new two-quadrant zero-voltage transition converter for DC motor drives, *International Journal of Electronics*, Vol. 86, 217-231, 1999.

Ching, T.W., and K. T. Chau, A new two-quadrant zero-current transition converter for DC motor drives, *International Journal of Electronics*, Vol. 88, 719-735, 2001.

Rajashekara, K., History of Electric Vehicles in General Motors, *IEEE Transactions on Industry Applications*, Vol. 30, 897-903, 1994.

(Received March 8, 2005; accepted May 18, 2005)